6.1 Coherence

W. Martienssen, H. Paul

6.1.1 Historical remarks

In its original meaning, coherence was just a synonym of ability to interfere. Two light beams were said to be (mutually) coherent, when they could be made to interfere, i.e. to produce an observable interference pattern. This requires the presence of field correlations on which a strict coherence concept therefore has to be based. Noteworthy are studies by Taylor [09Tay], who showed that an interference pattern can be observed at extremely low intensities, without loss of visibility, provided the exposition time is made long enough. Great progress came from the development of photoelectric detectors with very short resolving times which made it possible to observe not only spatial but also temporal interference (beating) [62Jav], and, moreover, both spatial and temporal intensity correlations. In their pioneering work, Brown and Twiss [56Bro] observed intensity correlations in star light, thus determining the angular diameter of fixed stars. Photomultipliers allowed to detect single photons, and hence to count photons [67Are] and detect photon coincidence counts [57Reb, 57Twi]. With the advent of the laser [60Mai, 61Jav] the experimenter had a new source producing light with unprecedented properties at hand. Relevant theoretical papers are Einstein's light-quanta hypothesis [1905Ein], his analysis of energy fluctuations in blackbody radiation [09Ein], von Laue's analysis of the degrees of freedom of light beams [14Lau], and Glauber's introduction of the concept of coherent states into the quantum theory of radiation [63Gla, 65Gla].

6.1.2 Basic concepts

6.1.2.1 Classical light

Classical light is a radiation field that can be correctly described classically in the sense that all quantum-mechanical field correlation functions can be exactly reproduced by classical averages. This condition is fulfilled when a positive-definite P function, as introduced by Glauber [65Gla], exists for the field in quantum-mechanical description, i.e., when the density operator for the field can be represented, in the Dirac formalism, as $\varrho = \int P(\alpha_1, \alpha_2, \dots) |\, \alpha_1 \rangle | \, \alpha_2 \rangle \dots \langle \, \alpha_2 \, | \langle \, \alpha_1 \, | \, \mathrm{d}^2\alpha_1 \, \mathrm{d}^2\alpha_2 \dots$ with $P(\alpha_1, \alpha_2, \dots) \geq 0$ ($|\, \alpha \rangle$: single-mode coherent state). Typical examples are chaotic, in particular thermal light and radiation from lasers as well as radio and radar transmitters. Chaotic light is produced by natural sources such as the sun or stars, or by any kind of conventional sources. The chaotic nature of the radiation is preserved when linear filters, e.g. apertures, spectral filters and polarizers, are applied.

6.1.2.2 Non-classical light

Non-classical light is a radiation field that has no positive-definite P representation. Another, however only sufficient, criterion is the appearance of negativities in the quantum-mechanical Wigner function of the field. Examples are fields with a fixed photon number, in particular the propagating wave packets generated in spontaneous emission (single photons) and parametric down-conversion (photon pairs, see Sect. 6.1.4.5), antibunched and squeezed light.

6.1.2.3 Field mode

A field mode is in its original meaning an eigenmode of a resonator, i.e. a monochromatic standing-wave field whose spatial distribution and frequency are determined by the resonator geometry; in a generalized sense a polarized, monochromatic field described by a special solution of Maxwell's equations, e.g. a traveling plane wave or a spherical wave. Formally, a field mode can be treated equivalently to a harmonic oscillator.

6.1.2.4 Single-mode field

A single-mode field is an excitation of a single mode of an optical resonator, or, more generally, the field within a single laser pulse or in a spatial–temporal region that can be identified with a coherence volume (see Sect. 6.1.3.2). The common property of single-mode fields is that they can be described by a single complex amplitude and, hence, have only one degree of freedom of motion.

6.1.2.5 Electric field strength

The Fourier representation of the electric field strength $E(\boldsymbol{r},t) = \int_{-\infty}^{+\infty} E(\boldsymbol{r},\nu)\mathrm{e}^{-2\pi\mathrm{i}\nu t}\mathrm{d}\nu$ can be written as

$$E(\boldsymbol{r},t) = E^{(+)}(\boldsymbol{r},t) + E^{(-)}(\boldsymbol{r},t)\ , \tag{6.1.1}$$

$$E^{(+)}(\boldsymbol{r},t) = \int_0^{+\infty} E(\boldsymbol{r},\nu)\mathrm{e}^{-2\pi\mathrm{i}\nu t}\mathrm{d}\nu\ ,\ E^{(-)}(\boldsymbol{r},t) = \int_0^{+\infty} E^*(\boldsymbol{r},\nu)\mathrm{e}^{2\pi\mathrm{i}\nu t}\mathrm{d}\nu\ , \tag{6.1.2}$$

where $E^{(+)}$ and $E^{(-)}$ are called *positive* and *negative frequency part of the electric field strength.* The former is known as *analytic signal* [91Bor]. In the quantum-mechanical description E, and consequently also $E^{(+)}$ and $E^{(-)}$, become operators, where $E^{(+)}$ contains only photon annihilation operators and $E^{(-)}$ only photon creation operators.

6.1.2.6 Interference

Optical interference results from a superposition of the electric field strengths of different beams. The production of an interference pattern in conventional interference experiments (diffraction, Young's double slit experiment or any kind of interferometer) requires a fixed phase difference between the beams involved to be maintained during the whole observation time.

6.1.2.7 Decoherence

Decoherence is destruction, caused by interaction with the environment, of phase relations that are present in quantum-mechanical superposition states. In particular, due to decoherence quantum-mechanical superpositions of states corresponding to macroscopically distinguishable properties evolve, at an extremely short time scale, into mixtures, which substantiates the classical reality concept. Since decoherence destroys entanglement (see Sect. 6.1.4.5) as well, it is detrimental in any process that might be used in quantum information transmission and processing, especially quantum computing.

6.1.3 Coherence theory

6.1.3.1 Field correlation functions

6.1.3.1.1 Definitions

In its general form, the n-th-order correlation function of an electromagnetic field is defined as

$$G^{(n)}(\boldsymbol{r}_1,t_1;\ldots;\boldsymbol{r}_{2n},t_{2n}) = \langle E^{(-)}(\boldsymbol{r}_1,t_1)\ldots\ E^{(-)}(\boldsymbol{r}_n,t_n)E^{(+)}(\boldsymbol{r}_{n+1},t_{n+1})\ldots\ E^{(+)}(\boldsymbol{r}_{2n},t_{2n})\rangle \quad (n=1,2,\ldots)\ , \tag{6.1.3}$$

where the bracket indicates an ensemble average in classical theory and the expectation value in quantum theory. In the quantum-mechanical description, $E^{(-)}$ and $E^{(+)}$ are noncommuting operators. In (6.1.3) they are written in the so-called normal order, which excludes vacuum contributions. The label n indicates the order of the correlation function (with respect to intensity). We follow here the notation that is customary in quantum optics. In classical optics, (6.1.3) is referred to as correlation function of $2n$-th order (with respect to field strength). Since in conventional interference experiments (apart from polarization interferometers) the polarization is irrelevant, the electric field strength is treated as a scalar. Alternatively, (6.1.3) applies to a linearly polarized field.

Of practical relevance are only the first-order correlation function

$$G^{(1)}(\boldsymbol{r}_1,\boldsymbol{r}_2;\tau) = \langle E^{(-)}(\boldsymbol{r}_1,t)E^{(+)}(\boldsymbol{r}_2,t+\tau)\rangle \tag{6.1.4}$$

(the special value $G^{(1)}(\boldsymbol{r},\boldsymbol{r};0)$ being the intensity at position $\boldsymbol{r}$) and the special second-order correlation function

$$G^{(2)}(\boldsymbol{r}_1,\boldsymbol{r}_2;\tau) = \langle E^{(-)}(\boldsymbol{r}_1,t)E^{(-)}(\boldsymbol{r}_2,t+\tau)E^{(+)}(\boldsymbol{r}_2,t+\tau)E^{(+)}(\boldsymbol{r}_1,t)\rangle \tag{6.1.5}$$

(the correlation between the intensities at space–time points $\boldsymbol{r}_1,t$ and $\boldsymbol{r}_2,t+\tau$). In both cases the field is assumed to be stationary. In these circumstances, making use of the ergodic hypothesis, the classical ensemble averages can be replaced by time averages. The time difference τ is referred to as the delay time. The modulus of (6.1.4) can be inferred from the intensity distribution in a conventional interference experiment (see Sect. 6.1.3.2), whereas (6.1.5) can be measured with two separate detectors (see Sect. 6.1.4.1 and Sect. 6.1.4.2).

6.1.3.1.2 Connections between correlation functions of different order

The stochastic nature of a chaotic field has the consequence that the full statistical information on it is already contained in its first-order correlation function. In fact, any higher-order correlation in chaotic fields can be expressed in terms of first-order correlation functions. In particular, the second-order correlation function (6.1.5) for chaotic light takes the form

$$G^{(2)}(\boldsymbol{r}_1, \boldsymbol{r}_2; \tau) = G^{(1)}(\boldsymbol{r}_1, \boldsymbol{r}_1; 0)\, G^{(1)}(\boldsymbol{r}_2, \boldsymbol{r}_2; 0) + \mid G^{(1)}(\boldsymbol{r}_1, \boldsymbol{r}_2; \tau) \mid^2 \ . \tag{6.1.6}$$

Equation (6.1.6) is the basis of stellar intensity interferometry (see Sect. 6.1.4.3).

6.1.3.2 First-order coherence

6.1.3.2.1 Degree of coherence

The quantitative description of interference is based on the first-order correlation function (6.1.4) which, apart from a factor, is just the interference term in the expression for the intensity at an observation point P. In a typical conventional interference experiment a primary beam is divided, by either beam splitting (with the help of a partly, normally semi-, reflecting mirror) or wave front splitting (provided by a screen with pinholes), into two partial beams which, after having propagated along different paths, are re-united on a detector surface. Tracing the two field strengths being superposed at P at a given instant back to the primary beam, one arrives, in general, at two space–time points $\boldsymbol{r}_1, t$ and $\boldsymbol{r}_2, t+\tau$. This explains why the correlations between those field strengths determine the visibility of the interference pattern (see (6.1.8)).

The normalized correlation function

$$g^{(1)}(\boldsymbol{r}_1, \boldsymbol{r}_2; \tau) = \frac{G^{(1)}(\boldsymbol{r}_1, \boldsymbol{r}_2; \tau)}{\sqrt{G^{(1)}(\boldsymbol{r}_1, \boldsymbol{r}_1; 0)}\sqrt{G^{(1)}(\boldsymbol{r}_2, \boldsymbol{r}_2; 0)}} \tag{6.1.7}$$

is referred to as the *complex degree of coherence*, and its modulus $\mid g^{(1)} \mid$ is called the *mutual degree of coherence* of the light oscillations at $\boldsymbol{r}_1$ and $\boldsymbol{r}_2$, with delay τ.

The degree of coherence determines the visibility v of the interference pattern through the relation [91Bor]

$$v = \frac{I_{\max} - I_{\min}}{I_{\max} + I_{\min}} = \frac{2\mu}{\mu^2 + 1} \mid g^{(1)}(\boldsymbol{r}_1, \boldsymbol{r}_2; \tau) \mid , \tag{6.1.8}$$

where μ^2 is the ratio of the intensities of the interfering beams at the observation point P, and $I_{\max}, I_{\min}$ are the maximum and minimum intensities in the interference pattern.

We speak of (*full*) *coherence*, when $\mid g^{(1)} \mid$ reaches its maximum value 1 (in that case the visibility takes its absolute maximum), of *partial coherence*, when $0 <\mid g^{(1)} \mid< 1$, and of *incoherence*, when $g^{(1)} = 0$.

6.1.3.2.2 Temporal coherence

Specializing to $\boldsymbol{r}_1 = \boldsymbol{r}_2$, the degree of coherence $\mid g^{(1)}(\boldsymbol{r}_1, \boldsymbol{r}_1; \tau) \mid$, as a function of τ, has its maximum (unity) at $\tau = 0$ and falls off for increasing $\mid \tau \mid$. Its effective width is called *coherence time* Δt_c. Usually, the root mean square (r.m.s.) width is taken as effective width [65Man, 95Man]. Since the Fourier transform of (6.1.4), at $\boldsymbol{r}_1 = \boldsymbol{r}_2$, with respect to τ gives us the power spectrum (spectral density) of the field (*Wiener–Khintchine theorem*), Δt_c and the line width (r.m.s. width) $\Delta\nu$ satisfy the relation

$$\Delta\nu \cdot \Delta t_\mathrm{c} \gtrsim 1 \ . \tag{6.1.9}$$

It follows: In a light field with line width $\Delta\nu$ interferences between partial beams having path differences $c\Delta t$ can be observed only when

$$\Delta t < \Delta t_c \quad \text{or} \quad \Delta\nu\Delta t < 1 . \tag{6.1.10}$$

The relations (6.1.10) are called *temporal coherence conditions*.

The distance over which the light propagates during the coherence time is called (*longitudinal*) *coherence length* Δl_c,

$$\Delta l_c = c\Delta t_c \approx c/\Delta\nu = \lambda_0^2/\Delta\lambda , \tag{6.1.11}$$

where λ_0 is the wavelength at the line center and $\Delta\lambda$ is the bandwidth expressed as a wavelength interval.

6.1.3.2.3 Spatial coherence

Specializing to $\tau = 0$, the function $| g^{(1)}(\boldsymbol{r}_1, \boldsymbol{r}_2; 0) |$, depending actually on $| \boldsymbol{r}_2 - \boldsymbol{r}_1 |$, drops from its maximum (unity) at $\boldsymbol{r}_1 = \boldsymbol{r}_2$ with growing values of $| \boldsymbol{r}_2 - \boldsymbol{r}_1 |$. The effective width of this function is called *transverse coherence length* $\Delta l_{c,\mathrm{trans}}$.

A rough estimate of $\Delta l_{c,\mathrm{trans}}$ is given by the formula [65Man, 95Man]

$$\Delta l_{c,\mathrm{trans}} \lesssim \lambda_0 R/\Delta x , \tag{6.1.12}$$

where Δx is the linear dimension (side of a square or diameter of a circle) of the quasimonochromatic chaotic source and R is the distance of the observation plane from the source. Equivalently, light from such a source with surface ΔA is said to be (spatially) coherent within a cone, with its center in the midst of the emitting surface and its axis approximately orthogonal to it, whose angular aperture $\Delta\gamma_c$ and solid angle $\Delta\Omega_c$ satisfy the equations

$$\Delta x \ \sin\Delta\gamma_c \lesssim \lambda_0 \quad \text{and} \quad \Delta A \cdot \Delta\Omega_c \lesssim \lambda_0^2 , \tag{6.1.13}$$

respectively. The angle $\Delta\gamma_c$, or the corresponding solid angle $\Delta\Omega_c$, is a natural measure of spatial coherence since, unlike $\Delta l_{c,\mathrm{trans}}$, it is independent of R. It follows: Interferences within a light field emitted from a surface with diameter Δx can be observed only within a beam with the angular aperture $\Delta\gamma$, where

$$\Delta\gamma < \Delta\gamma_c \quad \text{or} \quad \Delta x \ \sin\Delta\gamma < \lambda_0 . \tag{6.1.14}$$

The relations (6.1.14) are called *spatial coherence conditions*.

Equation (6.1.12) can be understood from the following argument: In a Young-type interference experiment, light from an extended chaotic source, after passing two pinholes in a screen, produces an interference pattern on a distant observation screen. Since different source points emit independently, they generate an individual interference pattern each. Those patterns are displaced with respect to each other. In order that they, nevertheless, add up to a visible interference pattern, the maximum displacement occurring must not reach the order of the fringe spacing. This requirement yields (6.1.12).

An accurate determination of the transverse coherence length is based on the *van Cittert–Zernike theorem* [34Cit, 38Zer] which relates the correlation function $G^{(1)}(\boldsymbol{r}_1, \boldsymbol{r}_2; 0)$ to the intensity distribution $I(\boldsymbol{r}')$ on the surface assumed to be a portion of a plane, of the spatially incoherent, quasimonochromatic light source in the form [65Man, 95Man]

$$G^{(1)}(\boldsymbol{r}_1, \boldsymbol{r}_2; 0) = \left(\frac{k_0}{2\pi}\right)^2 \int_\sigma I(\boldsymbol{r}') \frac{\mathrm{e}^{\mathrm{i}k_0(R_2 - R_1)}}{R_1 R_2} \mathrm{d}^2\boldsymbol{r}' . \tag{6.1.15}$$

Here, R_i is the distance from the point $\boldsymbol{r}'$ on the surface σ to the observation point $\boldsymbol{r}_i$ $(i = 1, 2)$, and k_0 is the wave number with respect to the line center. In the far-zone of the field, the integral

(6.1.15) can be solved analytically for the case of a uniformly emitting circular source of diameter Δx to yield [65Man, 91Bor, 95Man]

$$| g^{(1)}(\boldsymbol{r}_1, \boldsymbol{r}_2; 0) | = 2 \mid J_1(u)/u \mid , \; u = \frac{1}{2} k_0 \Delta x \mid \boldsymbol{r}_2 - \boldsymbol{r}_1 \mid / R \, . \tag{6.1.16}$$

Here, J_1 is the Bessel function of the first kind and the first order, and R is the distance between the surface σ and the observation plane which is assumed to be parallel to σ. Since the function $2J_1(u)/u$ drops from its maximum value 1 at $u = 0$ to 0.88 at $u = 1$, one can say that a circular area of diameter

$$d = 0.32\, \lambda_0 R / \Delta x \tag{6.1.17}$$

is illuminated "almost coherently" [91Bor]. Equation (6.1.17) quantifies the estimate (6.1.12) for the special case of a circular source.

A circle with the transverse coherence length $\Delta l_{\mathrm{c,trans}}$ as diameter is called *area of coherence* [91Bor]. Actually, this concept traces back to M. von Laue [14Lau], who speaks of "elementary areas illuminated independently of each other" and identifies their number in a strictly monochromatic, polarized light beam with the number of the degrees of freedom of that beam. The segment of a cone whose base is the coherence area and whose height is the longitudinal coherence length Δl_{c} is referred to as the *coherence volume* [95Man]. In a classical picture, the instantaneous values of both the amplitude and the phase are, to a good approximation, constant over a coherence volume. This justifies to look upon the field within a coherence volume as a single-mode field. Due to the dependence of the coherence area on the distance between source and observation plane the coherence volume (at any observation plane) is also dependent on this distance. The mean photon number $\bar{n}$ per coherence volume is called *degeneracy parameter* or *occupation number* (or *excitation*) of the corresponding mode. For radiation from black thermal sources (black-body radiation) $\bar{n}$ follows from Planck's radiation law to be given by

$$\bar{n} = \frac{1}{\mathrm{e}^{\frac{h\nu}{kT}} - 1} \tag{6.1.18}$$

(T: temperature, h: Planck's constant, k: Boltzmann's constant) and hence depends strongly on wavelength and temperature, as is illustrated in Fig. 6.1.1.

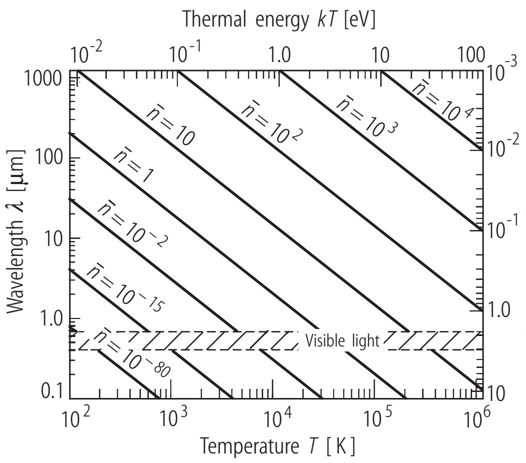

Fig. 6.1.1. Mean photon number $\bar{n}$ per mode (degeneracy parameter) for black-body radiation in dependence on wavelength and temperature. In the domain of visible radiation, for example, the figure shows the following: In order to achieve $\bar{n} = 10$, a black thermal source must be heated up to temperatures of some 100 000 K. At temperatures of the order of 1000 K typical of technical thermal sources, $\bar{n}$ attains only the order of 10^{-15}, even at the temperature of the sun's surface ($T = 5770$ K) $\bar{n}$ is still lower than 10^{-2}.

6.1.3.2.4 Filtering out coherent light from a chaotic source

The phrase "making (chaotic) light coherent" is used for making a coherently illuminated area or/and the coherence time in the field of a chaotic source sufficiently large, thus making the light more suitable for interference to be observed. In the case of spatial coherence this is achieved by reducing the effective size of the emitting surface. To this end, a secondary light source of small and perhaps adjustable dimensions is generated via imaging, with the help of a lens or a mirror, the primary source on a narrow-aperture diaphragm. In the case of temporal coherence it can be done by reducing the bandwidth with the help of a spectral filter.

6.1.3.2.5 Measurement of coherence lengths

The longitudinal coherence length Δl_{c} can be determined utilizing an interferometer, e.g. of Michelson's type. The path difference is gradually enlarged until the visibility vanishes. This critical path difference equals Δl_{c}. Similarly, the transverse coherence length $\Delta l_{\mathrm{c,trans}}$ can be measured in a Young's type interference experiment by increasing the distance of the pinholes in the screen or, equivalently, bringing the screen nearer to the source, until the interference pattern becomes invisible.

For the special case of light from fixed stars, whose transverse coherence length on earth attains several meters and even more, the screen with the two pinholes was replaced by two small mirrors, the light beams emerging from them being made to interfere (*Michelson's stellar interferometer*). From the critical distance of the mirrors d_{c} (corresponding to $u = 3.83$ in (6.1.16)), for which the visibility of the interference pattern becomes zero (for the first time), A.A. Michelson [21Mic] inferred the angular diameter of the star α with the help of the formula $d_{\mathrm{c}}\alpha = 1.22\lambda_0$ following from (6.1.16).

6.1.3.3 Laser light versus chaotic light

6.1.3.3.1 Generating mechanisms and radiation characteristics

6.1.3.3.1.1 Chaotic light

Chaotic light is generated by uncorrelated (spontaneous) emission from individual microscopic emitters, usually atoms or molecules. In a classical picture, the individual wave trains have random phases. Hence their superposition at a given position and a given time will randomly be constructive or destructive. As a result, the intensity exhibits strong fluctuations which give rise to characteristic intensity correlations (see Sects. 6.1.4.3 and 6.1.4.4). Under laboratory conditions the coherence volume of extended chaotic sources is rather small. For black-body radiation and for thermal light the degeneracy parameter $\bar{n}$ in the visible spectral range is by orders of magnitude smaller than unity (see Fig. 6.1.1).

6.1.3.3.1.2 Laser light

Laser light is generated by stimulated emission in a medium strongly pumped to produce population inversion, and placed within an optical resonator. Under these conditions, phase relations between the individual emitters are established so that the emitted waves interfere with each other. Only within a small aperture angle this interference is constructive and results in the emission of the coherent beam; in all other directions the interference turns out to be destructive, so that the entire emission is restricted to the coherent beam. The resonator gives rise to a very narrow bandwidth which can be reduced further, by orders of magnitude, by means of laser-frequency stabilization (locking the laser frequency to a narrow absorption line or a resonance line of a highly stabilized external resonator). Hence the coherence volume in cw laser fields is very large already at distances of a few meters; in pulsed lasers it coincides with the volume filled by a single pulse. The spectral density of the radiation power is extremely high, and the same holds for the degeneracy parameter. Qualitatively, laser light differs from chaotic light by its amplitude stabilization (see Sect. 6.1.4.4) resulting from a saturation mechanism in the generating process. Laser light, as well as the radiation from radar and radio transmitters, comes very close to the classical ideal of a monochromatic wave of fixed amplitude and phase.

6.1.3.3.2 Interference between beams from independent sources

Due to the small degeneracy parameter, any interference experiment performed with conventional light requires the observation time, or simply the exposition time of a photographic plate, to be much larger than the coherence time. The very large degeneracy parameter of laser light, on the contrary, makes it possible to detect interference even between beams from independently operated lasers (both cw and pulsed lasers), since the observation time can be chosen to be comparable with, or shorter than, the coherence time. For the first demonstration of this phenomenon [63Mag] pulsed lasers were used. Since the phases of pulses from different lasers are uncorrelated, the position of the interference pattern is random. This is in a marked contrast to conventional interference experiments, where the interfering beams are taken from the same source, so that the relative phases between them are determined solely by the geometry of the set-up.

Interference becomes possible even between strongly damped cw laser beams. This prediction relies on two basic theoretical results:

1. In the quantum-mechanical description, optimum interference (with visibility $v = 1$ for equal intensities) takes place between independent beams if, and only if, they are in a (quantum-mechanical) coherent state [63Gla], also named Glauber state, each [63Pau].
2. Absorption and reflection transform a Glauber state again into a Gauber state [64Bru, 65Bru]. In the actual interference experiment Radloff [71Rad], following a suggestion by Paul et al. [65Pau], utilized the intense laser beams off which the interfering beams were split by means of very weakly reflecting beam splitters, to control, via a shutter, the relative phase between the interfering beams.

6.1.3.3.3 Coherent interaction

Unlike chaotic light, laser light can be used to observe coherent interaction between light and matter. It is based on the fact that resonant intense coherent light induces on an atom or a molecule dipole oscillations whose phase is determined by the field phase. Hence in an atomic or molecular ensemble those individual dipole oscillations add up to a macroscopic (oscillating) polarization of the medium which, in turn, acts as a source of radiation. Examples of those processes are free induction decay, optical nutation, photon echo and self-induced transparency, as well as Coherent Stokes Raman Scattering (CSRS) and Coherent Antistokes Raman Scattering (CARS) (cf. [84She]).

6.1.3.4 Particle interference

Optical interference can be described equally well in the photon picture that dates back to Einstein [1905Ein]. Photons are particles with energy $E = h\nu$ (h: Planck's constant) and momentum $\boldsymbol{p} = (h/2\pi)\boldsymbol{k}$ ($\boldsymbol{k}$: wave vector). Equation (6.1.9) is tantamount to the quantum-mechanical time–energy uncertainty relation[1] $\Delta E \cdot \Delta t \geq h/4\pi$. Equation (6.1.13) can be based on Heisenberg's uncertainty relation for position and momentum of a particle, $\Delta x \cdot \Delta p \geq h/4\pi$. Applied to a photon, the latter states that a photon whose position is confined to the finite surface of the source with dimension Δx has a minimum momentum uncertainty with respect to the x direction, which defines a minimum angular aperture to be identified with $\Delta\gamma_c$ in (6.1.13).

Also massive particles possess wave properties (wave–particle dualism) resulting in interference phenomena. The analog of the optical wavelength is the de Broglie wavelength $\Lambda = h/mv$ (m: mass and v: velocity of the particle). It follows from this formula that interference can be observed only on particles with a small mass such as electrons, neutrons, atoms, molecules or clusters. While electron interference is known since 1927, atom optics has been established as a new discipline only recently. In fact, atom-optical analogs of optical elements, in particular beam splitters, are nowadays available.

Particle interference must always be interpreted as "interference of the particle with itself", as Dirac put it [58Dir]. In order to detect an interference pattern, the observation has to be carried out on an ensemble being in a pure quantum state with respect to the motional degrees of freedom, i.e. being described by a well-defined wave function. In the quantum-mechanical description, interference takes place, on a detector surface, between the probability amplitudes that correspond to different paths the particle is allowed to take. There exists a complementarity between the visibility of the interference pattern and the information on the particle's path. In particular, maximum visibility requires the path to be completely undetermined. In this context atoms or molecules are especially attractive because of their internal degrees of freedom that can be utilized to mark the particle's path, e.g. by excitation of an electronic level followed by spontaneous emission or via coherent excitation of hyperfine levels [98Due], which makes the interference pattern disappear.

6.1.3.5 Higher-order coherence

While first-order coherence underlies the conventional interference experiments resulting in the appearance of a visible interference pattern, Glauber [65Gla] generalized the coherence concept with regard to photon coincidence measurements to be carried out with two or more detectors. He termed a field *coherent in M-th order*, when the normalized correlation functions

$$\begin{aligned} &g^{(n)}(\boldsymbol{r}_1, t_1; \ldots; \boldsymbol{r}_n, t_n; \boldsymbol{r}_{n+1}, t_{n+1}; \ldots; \boldsymbol{r}_{2n}, t_{2n}) \\ &\quad = \frac{G^{(n)}(\boldsymbol{r}_1, t_1; \ldots; \boldsymbol{r}_n, t_n; \boldsymbol{r}_{n+1}, t_{n+1}; \ldots; \boldsymbol{r}_{2n}, t_{2n})}{\sqrt{G^{(1)}(\boldsymbol{r}_1, t_1; \boldsymbol{r}_1, t_1)} \ldots \sqrt{G^{(1)}(\boldsymbol{r}_{2n}, t_{2n}; \boldsymbol{r}_{2n}, t_{2n})}} \end{aligned} \tag{6.1.19}$$

have modulus 1 for, and only for, all $n \leq M$. Evidently, this condition implies the relations

$$G^{(n)}(\boldsymbol{r}_1, t_1; \ldots; \boldsymbol{r}_n, t_n; \boldsymbol{r}_n, t_n; \ldots; \boldsymbol{r}_1, t_1) = G^{(1)}(\boldsymbol{r}_1, t_1; \boldsymbol{r}_1, t_1) \ldots G^{(1)}(\boldsymbol{r}_n, t_n; \boldsymbol{r}_n, t_n) \tag{6.1.20}$$

for all $n \leq M$. Physically, this means that the n-fold coincidence counting rate factorizes into the single counting rates which would be measured by each detector individually in the absence of all others. In other words, the detectors respond to the field in a statistically independent way. Hence

[1] Though the time–energy uncertainty relation is less fundamental than Heisenberg's uncertainty relation, since there exists no time operator, it is nevertheless very useful in spectroscopy [54Hei]. Then ΔE is interpreted as the accuracy of an energy measurement and Δt as the measurement time.

Glauber's higher-order coherence is characterized by the *absence* of *systematic* coincidences, when measurements on the radiation field are carried out with several independent detectors.

For chaotic light, (6.1.20) is not fulfilled already for $n = 2$ (see (6.1.6)). Hence this kind of light has only first-order coherence. Ideal laser light, on the other hand, is coherent in ∞-th order.

The coherence condition (6.1.20) aims at fields that are laser-like only up to a certain order, and, hence, in a sense interpolate between chaotic and laser light. Since, however, no such fields are known to date, the concept of higher-order coherence has hitherto found only little practical use.

6.1.4 Intensity interference

6.1.4.1 Formal description

Intensity interference is based on measurement of intensity correlations. The latter are described by the special second-order correlation function $G^{(2)}(\boldsymbol{r}_1, \boldsymbol{r}_2; \tau)$ (see (6.1.5)). Apart from a factor, this function has the physical meaning of the (conditional) probability that a photodetector at position $\boldsymbol{r}_2$ will click at time $t+\tau$, on condition that a photodetector at $\boldsymbol{r}_1$ has clicked at t [65Gla]. Accordingly, the delayed coincidence counting rate is proportional to $G^{(2)}(\boldsymbol{r}_1, \boldsymbol{r}_2; \tau)$.

6.1.4.2 Measurement

The intensity correlation function for zero delay time can be measured by correlating electronically the photocurrents from two detectors placed at different positions. To this end, the photocurrents are multiplied and, after narrow-band amplification, averaged over time. A second technique is to use two separate photocounters and single out electronically those events where a click from one detector is followed, within a narrow time window, by a click from the other. To account for non-zero delay time, a delay is introduced between the photocurrents in the first case. In the second case use is often made of time-to-digital converters.

6.1.4.3 Spatial intensity correlations

6.1.4.3.1 Stellar intensity interferometry

Equation (6.1.6), for $\tau = 0$, means for astronomy that measuring intensity correlations yields precisely the same information (the modulus of the first-order correlation function) as Michelson's stellar interferometer. The pioneering work was devised and carried out by Brown and Twiss [56Bro, 64Bro], who observed a drop of the intensity correlations to a constant level with increasing distance $\mid \boldsymbol{r}_2 - \boldsymbol{r}_1 \mid$ of the reflectors focusing light from the star on individual photomultipliers. This technique has two important advantages:

1. One gets rid of the disturbing influence of atmospheric scintillations, and
2. no mechanical connection of the reflectors is needed any longer, which allows to drastically enhance the detector distance.

6.1.4.4 Temporal intensity correlations

Delayed coincidences at a given position ($\boldsymbol{r}_1 = \boldsymbol{r}_2$) are measured with the following set-up [57Reb, 57Twi]: The incoming light is divided, with the help of a semitransparent beam splitter, into two beams each of which is directed to a separate photodetector. With the detectors being in equivalent positions, one solves in this way the problem of placing two detectors at the same position.

6.1.4.4.1 Amplitude stabilization

In contrast to chaotic radiation, light from a single-mode laser operated well above threshold is amplitude-stabilized. This means that the intensity correlation function, to a good approximation, satisfies the relation

$$G^{(2)}(\boldsymbol{r}_1, \boldsymbol{r}_1; \tau) = \left[G^{(1)}(\boldsymbol{r}_1, \boldsymbol{r}_1; \tau)\right]^2 \quad \text{for all } \tau \,. \tag{6.1.21}$$

6.1.4.4.2 Photon bunching

It follows from (6.1.6), for $\boldsymbol{r}_1 = \boldsymbol{r}_2$, that the delayed coincidence counting rate for chaotic light is distinctly enhanced at $\tau = 0$ compared to its values at delay times that are comparable to, or larger than, the coherence time (for an experimental demonstration see e.g. [69Foo]). This indicates from the viewpoint of classical optics the presence of strong intensity (or, equivalently, amplitude) fluctuations, and from the viewpoint of quantum optics a tendency for photons to arrive in bunches. Accordingly, this effect has been termed *photon bunching.*

Similar to the spatial case, the modulus of the first-order correlation function $G^{(1)}(\boldsymbol{r}_1, \boldsymbol{r}_1; \tau)$ can be found from the measurement of temporal intensity correlations. In particular, the coherence time can be inferred from the drop of the intensity correlation to a constant level with increasing delay time τ. In view of (6.1.9), this opens a way to indirectly measure very narrow bandwidths. In fact, the scheme, unlike conventional spectroscopy, works the better, the narrower the bandwidth.

Unfortunately, the coherence time attainable with thermal sources is normally still short in comparison to the response time of photodetectors, which practically prohibits the observation of photon bunching. However, laser light scattered from a moving ground glass [64Mar], from moving centers suspended in a fluid, or from inhomogeneities due to temperature fluctuations in a fluid, has stochastic character and, moreover, possesses the desired small bandwidth. Diffusion coefficients [69Foo] and the thermal conductivity were determined in this way.

6.1.4.4.3 Photon antibunching

Whereas in classical statistics any autocorrelation function has an absolute maximum at zero delay time, quantum states of the electromagnetic field were specified whose delayed coincidence counting rate exhibits a dip at $\tau = 0$. This intrinsically quantum-mechanical effect is known as *photon antibunching*, and light showing it falls therefore in the category of *non-classical light.*

The antibunching effect is observed in resonance fluorescence on single atoms. The underlying physical mechanism is as follows: An atomic system driven by a strong resonant field (laser field) becomes excited at a time and hence emits a photon. However, it cannot emit a second photon immediately afterwards, since the laser field needs some time to excite it again. So one will never register coincidences at zero delay time, in contrast to the situation at larger delay times. One of the main experimental problems is to ensure that actually one atom, at most, is under observation at a time. In their pioneering work, Kimble et al. [77Kim] worked with a very thin beam of sodium atoms, of which only a small section was observed. In these circumstances, it could not be excluded, however, that sometimes the observation volume was occupied by more than one atom. Nevertheless, a distinct dip in the intensity correlation function at $\tau = 0$ was observed. In later experiments, this handicap was overcome by studying resonance fluorescence on single ions stored in electromagnetic traps, or single molecules doped as impurities in solids or placed in a microcavity [98Kit].

6.1.4.5 Experiments with entangled photon pairs

6.1.4.5.1 Parametric down-conversion

One of the most puzzling quantum-mechanical features is entanglement (see also Sect. 5.1.9.3). Having no classical analog, it lies at the heart of the Einstein Podolsky Rosen (EPR) paradox [35Ein] and underlies any experiment designed to demonstrate a violation of Bell's inequalities (see also Sect. 5.1.9.4). By definition, a (pure) entangled state of two or more physical systems is described by an unfactorable wave function. Of special relevance are entangled states of two particles (labeled 1 and 2) for which a global variable $v = v_1 + v_2$, e.g. energy or spin, has a sharp value, whereas v_1 and v_2 are uncertain. Hence measuring v_1 fixes also v_2, even when particle 2 has traveled far away.

A very effective, widely used technique to generate entanglement is spontaneous parametric down-conversion. In this process, an intense laser beam is sent, as a pump, in a nonlinear crystal, which leads to a sporadic "decay" of a pump photon into a photon pair named signal and idler photon. Energy conservation requires the sum of the signal and the idler frequency to coincide with the pump frequency, and the phase matching condition implies a similar requirement for the wave vectors resulting in different propagation directions for the two photons. Moreover, whereas the time at which such an event occurs is impredictable over a comparatively long period, the possible delay between the emission of the signal and the idler photon is extremely short.

As a result of the frequency condition mentioned, a new coherence length determined by the large coherence length of the pump and hence much longer than the one-photon coherence lengths for signal and idler, becomes manifest in suitable experiments, which has to be assigned to the two-photon wave packet (sometimes called *biphoton*) as a whole.

6.1.4.5.2 Two-photon mixing

6.1.4.5.2.1 Hong–Ou–Mandel interferometer

When two photons are mixed at a 50% : 50% beam splitter, they leave it both in one or the other of the two output channels, provided they have arrived simultaneously at the beam splitter [87Fea, 87Hon]. The pioneering experiment [87Hon] was performed on photon pairs produced in spontaneous parametric down-conversion. The coincidence counting rate of detectors placed in the two output channels was observed to exhibit a distinct dip reaching almost zero, for zero delay time. Actually, this destructive interference is not bound to entanglement [87Fea]. Experimentally, this was shown by Rarity et al. [96Rar], who mixed a photon produced in spontaneous parametric down-conversion and a highly attenuated pulse from the pump laser.

The Hong–Ou–Mandel experiment [87Hon] was recently modified [98Str] by inserting in the signal channel a rod of birefringent material followed by a linear polarizer. This set-up allows the signal photon to propagate along two ways that differ in their optical path lengths by $2\Delta L$. The latter quantity being chosen much greater than the coherence length for both the signal and the idler photon, the signal photon was divided into two well-separated wave packets. Positioning the mirror such that the idler photon arrived precisely midway between the two signal wave packets, and afterwards varying ΔL with the help of a Pockels cell, the authors observed a sinusoidal change in the coincidence counting rate registered with a time window much greater than the delay between the two signal wave packets, and hence a transition from the dip in the Hong–Ou–Mandel experiment to a peak. Since signal and idler wave packets do not overlap at the beam splitter, this effect is clearly of non-classical origin.

6.1.4.5.3 Photon-pair interference

6.1.4.5.3.1 Interferometric devices

Photon pairs generated in spontaneous parametric down-conversion are sent into one entrance channel of a Michelson interferometer, and the transmitted light is detected by a "photon-pair detector" consisting of a semitransparent beam splitter with a separate detector in each output channel [89Moh, 90Kwi, 91Bre]. The coincidence counting rate observed with a very narrow time window, as a function of the path difference of the interferometer arms, displays interference fringes corresponding to a de Broglie wavelength that is given by the wavelength of the pump [90Kwi, 91Bre]. The corresponding second-order coherence time is much longer than the first-order coherence time of the signal and the idler photon. The described interference phenomenon results from the superposition of the probability amplitudes for the following two cases:

1. Both photons went through the short arm of the interferometer, and
2. both photons went through the long arm.

Those two cases cannot be distinguished due to the uncertainty of the emission time of the photon pair. Hence, what is observed is interference of the photon pair (biphoton) with itself. The fringe visibility of 87% measured in [91Bre] distinctly exceeded the critical value of 50% compatible with a classical model.

A similar investigation was recently carried out with a Young double-slit set-up [99Fon]. Further, it should be mentioned that Jacobson et al. [95Jac] proposed a modified Mach–Zehnder interferometer that is capable of measuring the de Broglie wavelength of a multiphoton wave packet.

6.1.4.5.3.2 Franson experiment

Following a proposal by Franson [89Fra], Kwiat et al. [93Kwi] performed the following experiment: The two photons of a pair generated in spontaneous parametric down-conversion are coupled each into a separate Mach–Zehnder interferometer. Exiting the interferometer, the photons fall on separate detectors whose coincidence counts are registered. The experimental parameters are chosen such that only two types of events are observed:

1. Both photons take the long way in the respective interferometer, and
2. both take the short way.

Since the emission time of the photon pair is uncertain, the detectors cannot distinguish those two cases, which gives rise to the occurrence of interference fringes in the coincidence counting rate, as a function of an additional path difference introduced in one of the interferometers by translating the right-angle prism. The measured fringe visibility of about 80% indicated a strong violation of Bell's inequality.

6.1.5 Photon counting statistics

6.1.5.1 Measurement

The field is made to impinge on a single photodetector. Confining the illumination, with the help of a pinhole placed in front of the detector, to a coherence area ΔA_c and registering the photoelectrons (clicks) over a time interval that equals the coherence time Δt_c, one counts the photons contained in a coherence volume.

6.1.5.2 Photon distribution functions

For chaotic light the probability p_n to detect just n photons is given by the distribution

$$p_n = \frac{\overline{n}^n}{(\overline{n}+1)^{n+1}} \quad (\textit{Bose–Einstein distribution}) \,, \tag{6.1.22}$$

where $\overline{n}$ is the mean photon number per coherence volume. For (ideal) laser light the corresponding probability is given by the distribution

$$p_n = \frac{\exp(-\overline{n})\,\overline{n}^n}{n!} \quad (\textit{Poisson distribution}) \,. \tag{6.1.23}$$

Both distributions are shown in Fig. 6.1.2 for two values of $\bar{n}$.

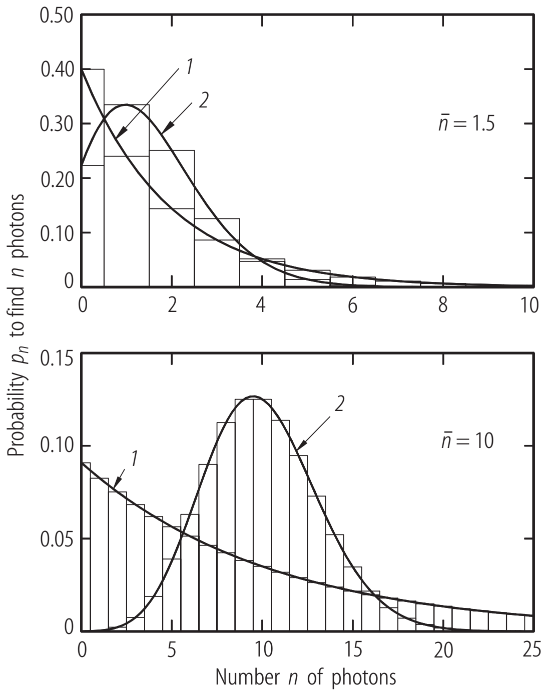

Fig. 6.1.2. Bose–Einstein distribution (*1*) and Poisson distribution (*2*) for a mean photon number of $\bar{n} = 1.5$ and $\overline{n} = 10$. The figure indicates that already for moderate mean photon numbers the two distributions differ distinctly in both their shape and the positions of their maxima, whereas for $\bar{n} \lesssim 1$ they are hard to discriminate experimentally.

6.1.5.3 Measurements under different experimental conditions

Measurements of this kind are also performed under different experimental conditions. When the illuminated area ΔA_{ill} is chosen smaller than ΔA_{c} or/and the observation time Δt_{obs} shorter than Δt_{c}, the distributions (6.1.22) and (6.1.23) are still valid. (Only the mean photon numbers, referring to the actual observation volume, change.) For growing ΔA_{ill} ($> \Delta A_{\mathrm{c}}$) or/and Δt_{obs} ($> \Delta t_{\mathrm{c}}$) the photon distribution for chaotic light tends to a Poisson distribution, while the distribution for laser light remains Poissonian.

The Bose–Einstein distribution was first measured on laser light scattered from a suspension of polysterene globules [67Are]. Probability densities for the intensity of pseudothermal light [65Man] were measured already before [66Mar1, 66Mar2].

6.1.5.4 Variances of the photon number

The variances of the photon number follow from (6.1.22) and (6.1.23) to be

$$\Delta n^2 = \overline{n^2} - \overline{n}^2 = \overline{n}^2 + \overline{n} \quad \text{for chaotic light}\ , \tag{6.1.24}$$

and

$$\Delta n^2 = \overline{n} \quad \text{for (ideal) laser light}\ . \tag{6.1.25}$$

Evidently, the Bose–Einstein distribution is broader, for equal average photon numbers $\overline{n}$, than the Poisson distribution. Hence the former falls in the category of *super-Poissonian statistics*. Antibunched light, on the other hand, normally exhibits a photon distribution that is narrower than the Poisson distribution – accordingly one speaks of *sub-Poissonian statistics* – , and the variance of the photon number is smaller than $\overline{n}$. Equivalently, the so-called *Q parameter* introduced by Mandel [79Man], see also Sect. 5.1.3.6.1, $Q = (\Delta n^2 - \overline{n})/\overline{n}$, being equal to zero for Poissonian statistics and positive for super-Poissonian statistics, becomes negative for sub-Poissonian statistics.

References for 6.1

1905Ein Einstein, A.: Ann. Physik (Leipzig) **17** (1905).

09Ein Einstein, A.: Phys. Z. **10** (1909) 185.
09Tay Taylor, G.I.: Proc. Cambridge Philos. Soc. **15** (1909) 114.

14Lau Laue, M. von: Ann. Phys. (Leipzig) **44** (1914) 1197.

21Mic Michelson, A.A., Pease, F.G.: Astrophys. J. **53** (1921) 249.

34Cit Cittert, P.H. van: Physica **1** (1934) 201.

35Ein Einstein, A., Podolsky, B., Rosen, N.: Phys. Rev. **47** (1935) 777.

38Zer Zernike, F.: Physica **5** (1938) 785.

54Hei Heitler, W.: The quantum theory of radiation, 3rd ed., London: Oxford University Press, 1954.

56Bro Brown, R.Hanbury, Twiss, R.Q.: Nature (London) **178** (1956) 1046.

57Reb Rebka, G.A., Pound, R.V.: Nature (London) **180** (1957) 1035.
57Twi Twiss, R.Q., Little, A.G., Brown, R.Hanbury: Nature (London) **180** (1957) 324.

58Dir Dirac, P.A.M.: The principles of quantummechanics, 4th ed., London: Oxford University Press, 1958.

60Mai Maiman, T.H.: Nature (London) **187** (1960) 493.

61Jav Javan, A., Bennett, W.R., Herriott, D.R.: Phys. Rev. Lett. **6** (1961) 106.

62Jav Javan, A., Ballik, E.A., Bond, W.L.: J. Opt. Soc. Am. **52** (1962) 96.

63Gla Glauber, R.J.: Phys. Rev. **131** (1963) 2766.
63Mag Magyar, G., Mandel, L.: Nature (London) **198** (1963) 255.
63Pau Paul, H., Brunner, W., Richter, G.: Ann. Phys. (Leipzig) **12** (1963) 325.

64Bro Brown, R.Hanbury: Sky Telesc. **28** (1964) 64.
64Bru Brunner, W., Paul, H., Richter, G.: Ann. Phys. (Leipzig) **14** (1964) 384.
64Mar Martienssen, W., Spiller, E.: Am. J. Phys. **32** (1964) 919.

65Bru Brunner, W., Paul, H., Richter, G.: Ann. Phys. (Leipzig) **15** (1965) 17.
65Gla Glauber, R.J., in: Qantum optics and electronics, DeWitt C., Blandin, A., Cohen-Tannoudji, C. (eds.), New York: Gordon and Breach, 1965.
65Man Mandel, L., Wolf, E.: Rev. Mod. Phys. **37** (1965) 231.
65Pau Paul, H., Brunner, W., Richter, G.: Ann. Phys. (Leipzig) **16** (1965) 93.

66Mar1 Martienssen, W., Spiller, E.: Phys. Rev. **145** (1966) 285.
66Mar2 Martienssen, W., Spiller, E.: Phys. Rev. Lett. **16** (1966) 531.

67Are Arecchi, F.T., Giglio, M., Tartari, U.: Phys. Rev. **163** (1967) 186.

69Foo Foord, R., Jakeman, E., Jones, R., Oliver,C.J., Pike, E.R.: IERE Conf. Proc. **14** (1969).

71Rad Radloff, W.: Ann. Phys. (Leipzig) **26** (1971) 178.

77Kim Kimble, H.J., Dagenais, J.M., Mandel, L.: Phys. Rev. Lett. **39** (1977) 691.

79Man Mandel, L.: Opt. Lett. **4** (1979) 205.

84She Shen,Y.R.: The principles of nonlinear optics, New York: Wiley, 1984.

87Fea Fearn, H., Loudon, R.: Opt. Commun. **64** (1987) 485.
87Hon Hong, C.K., Ou, Z.Y., Mandel, L.: Phys. Rev. Lett. **59** (1987) 2044.

89Fra Franson, J.D.: Phys. Rev. Lett. **62** (1989) 2205.
89Moh Mohler, E., Brendel, J., Lange, R., Martienssen, W.: Europhys. Lett. **8** (1989) 511.

90Kwi Kwiat, P.G., Vareka, W.A., Hong, C.K., Nathel, H., Chiao, R.Y.: Phys. Rev. A **41** (1990) 2910.

91Bor Born, M., Wolf, E.: Principles of optics, 6th ed., Oxford: Pergamon Press, 1991.
91Bre Brendel, J., Mohler, E., Martienssen, W.: Phys. Rev. Lett. **66** (1991) 1142.

93Kwi Kwiat, P.G., Steinberg, A.M., Ciao, R.Y.: Phys. Rev. A **47** (1993) R2472.

95Jac Jacobson, J., Björk, G., Chuang, I., Yamamoto, Y.: Phys. Rev. Lett. **74** (1995) 4835.
95Man Mandel, L., Wolf, E.: Optical coherence and quantum optics, Cambridge: Cambridge University Press, 1995.

96Rar Rarity, J.G., Tapster, P.R., Loudon, R., in: Quantum interferometry, DeMartini, F., Denardo, G., Shih, Y. (eds.), Weinheim: VCH, 1996.

98Due Dürr, S., Nonn, T., Rempe, G.: Nature (London) **395** (1998) 33.
98Kit Kitson, S.C., Jonsson, P., Rarity, J.G., Tapster, P.R.: Phys. Rev. **58** (1998) 620.
98Str Strekalov, D.V., Pittman, T.B., Shih, Y.H.: Phys. Rev. A **57** (1998) 567.

99Fon Fonseca, E.J.S., Monken, C.H., Pádua, S.: Phys. Rev. Lett. **82** (1999) 2868.